

*Iranian Journal of Oil & Gas Science and Technology*, Vol. 10 (2021), No. 3, pp. 20–38  
<http://ijogst.put.ac.ir>

## Experimental Investigation of Permeability Reduction Due to Migration of Non-swelling Clay Minerals

Siavash Ashoori<sup>1\*</sup>, Ehsan Safavi<sup>2</sup>, Jamshid Moghaddasi<sup>1</sup>, and Parvin Kolahkaj<sup>2</sup>

<sup>1</sup> Associate Professor, Department of Petroleum Engineering, Petroleum University of Technology, Ahwaz, Iran

<sup>2</sup> M.S. Student, Department of Petroleum Engineering, Petroleum University of Technology, Ahwaz, Iran

### Highlights

- The effects of non-swelling clay minerals motions on permeability;
- The motion of fine particles under various pressure differences, flow rates, and concentrations;
- Specifying the critical flow rate for destroying the clay bridges;
- Permeability reduction and formation damage are proportional to the concentration of particles and the inverse of glass bead size

*Received:* February 17, 2021; *revised:* July 07, 2021; *accepted:* July 14, 2021


### Abstract

Formation damage is reported during the secondary and tertiary stages of reservoir lifespan. One of the unpleasant sequences of formation damage caused by fine particles is permeability reduction due to pore plugging and bridging. The fine particles might exist initially in a porous medium or be introduced by external sources. In addition, there is a variety of particle types and sizes. The current research focuses on the effects of non-swelling clay minerals motions, such as the laminar ones found in Iranian sandstone reservoirs, on permeability. For this purpose, sand packs in various glass bead sizes and containing aluminum oxide as fine particles were designed to scrutinize the motion of fine particles under various pressure differences, flow rates, and concentrations. It was concluded that for each of the three sand packs regarded as the porous media in this study and composed of fine glass beads with different sizes, there is a critical flow rate as a function of glass bead size. For the flow rates lower than the critical flow rate, bridges form stably and lead to the most severe formation damage. After reaching the critical flow rate, the bridges weaken and break, and relative permeability will be independent of the flow rate. It was deduced that permeability reduction and formation damage are directly proportional to particle concentration and inversely proportional to glass bead size.

**Keywords:** Critical flow rate, Fine migration, Formation damage, Permeability reduction

### How to cite this article

Ashoori, S., Safavi, E., Moghaddasi, and J., Kolahkaj, P., *Experimental Investigation of Permeability Reduction Due to Migration of Non-swelling Clay Minerals*, *Iran J. Oil Gas Sci. Technol.*, Vol. 10, No. 3, pp. 20–38, 2021.

DOI: <http://dx.doi.org/10.22050/ijogst.2021.133602>. This is an Open Access article under Creative Commons Attribution 4.0 International License. ([creativecommons.org/licenses/by/4.0](http://creativecommons.org/licenses/by/4.0)) 

## 1. Introduction

Due to high energy demand, secondary and tertiary recovery (or enhanced oil recovery, EOR) methods are applied to the reservoirs (Green and Willhite 1998; Fanchi 2006). As the oldest secondary recovery

\* Corresponding author:

Email: [ashoori@put.ac.ir](mailto:ashoori@put.ac.ir)

method, waterflooding is the most common approach to maintaining reservoir pressure and sweeping trapped oil because water is available and inexpensive. During the EOR stage, water-based solutions are injected into the reservoir to change the reservoir fluid and rock characteristics. Meanwhile, permeability reduction is sometimes an inevitable consequence. Several reasons contribute to permeability reduction, such as migration of fine particles, clay swelling, and mineral dissolution and participation. In addition, geomechanical deformation and external solid particles associated with the injected solution might cause a drastic decrease in reservoir permeability and diminish well injectivity.

Waterflooding injects water into the reservoir to extract residual oil (Gulick and McCain, 1998). The waterflooding process was discovered inadvertently more than 100 years ago (Terry et al., 2015). Attentions were directed to the waterflooding in the late 1940s and early 1950s, when reservoirs approached their economic limits, and operators were obligated to increase production (Willhite, 1986). Waterflooding is the first method, usually applied right after the primary recovery phase, and this proven method is beneficial in terms of feasibility and economics. One inevitable challenge associated with this method is the migration of fine particles due to applied drag force by the injected fluid, especially in argillaceous sandstone formations, causing permeability reduction and a radical increase in pressure drop. In many geothermal doublet projects, even the filtration of formation brine before reinjecting it into the reservoir does not address the problem (Satman, 2011). In Siri offshore field in the Persian Gulf, water injection with a rate of 9100 bbl/day was employed to maintain reservoir pressure and increase oil recovery since 1984. After that, well injectivity diminished enormously to 2200 bb/day; hence, the project was stopped in 1990. This formation damage was due to the migration and aggregation of the suspended particles within the reservoir (Moghadasi et al., 2002; 2003; 2004).

Li and Prigioble (2018) developed a numerical model employing the lattice Boltzmann method to study migration of fine particles in porous media on a microscopic scale. They concluded that particle size and the structure of porous media both affect the migration of fine particles. Pore plugging diverts the fluid flow, decreasing the permeability of the porous medium but increasing the pressure drop. Unexpectedly, this might cause an increase in the swept area and the oil recovery. Sazali et al. (2020) investigated the influential factors contributing to fine particle migration for the Sarawak field in Malaysia. The experimental results determined the critical flow rates at which fine particles start their motion. Sand production can be a remedy through different approaches. For instance, to prevent acceptable migration, the fluid injection rate must be smaller than the critical rate in which fine particles start to move due to the applied drag force (Karazincir et al., 2017). In addition, injecting chemical agents such as furan resin and silicate non-polymer material into unconsolidated porous medium to bond grains together and fix the particles in their places prevents sand production with produced fluid, as mentioned in the manuscript. It is worth mentioning that selected chemical material must cause the minimum permeability reduction (Alakbari et al., 2020). Galal et al. (2016) worked on appropriate remedies to formation damage due to fine particle migration. They employed different methods such as well testing and well performance analyses to identify and measure formation damage. In addition, laboratory tests had been performed to recognize the extension of damage and the efficiency of acidizing.

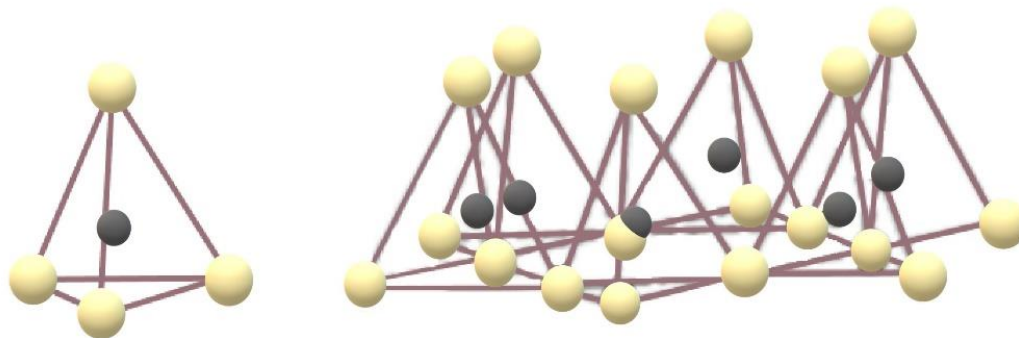
If pore throats of porous media are smaller than fine particle size, the migration of particles that existed in injected fluid might cause pore plugging and consequently permeability reduction. In addition, an increase in the concentration of fine particles intensifies formation damage (Wright and Chilingarian, 1989). Geomechanical deformations and chemical interactions are considered other formation damage sources (Muecke, 1979). Although glass beads and fine particles are assumed to be inert in this paper, the migration of fine particles as a geomechanical effect can still cause damage.

Despite that, several conducted studies pinpoint the role of clay swelling in permeability reduction during water injection. Hence, permeability degradation, especially in sandstone reservoirs, could be attributed to the migration of fine particles and clay swelling. Adsorption of polar components of oil by clay particles placed on the rock surface causes wettability alteration towards oil-wet, which counts as a negative impact on oil recovery by conventional water injection (Rezaei Gomari and Joseph, 2017). Sharifipour et al. (2017) investigated the influence of clay swelling on the oil recovery factor on a microscopic scale. They used sodium bentonite in a clay-coated micromodel and the image processing technique to evaluate the ultimate oil recovery factors after the injection of low-salinity water (LSW) and high-salinity water (HSW).

This study aims to recognize the reasons for formation damage assisted by monitoring the alteration of factors related to the displacement of the solid particle in porous media. The concerned parameters in this study are the flow rate, the initial concentration of particles in the porous medium, and glass bead size.

## 2. Theory

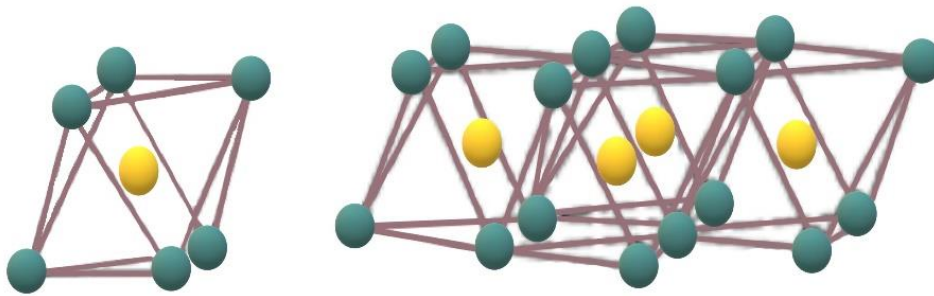
Clays minerals, which are only a few microns in thickness and composed of two or more layers, can adsorb water and swell to large particles. Clays, i.e., hydrated aluminum silicates, composed of alternating layers of alumina and silica, can be categorized based on properties such as cation exchange capacity (CEC) and water electrolytic arrangement. The most important clays in terms of their CEC are kaolinites (3–15 MEQ/100g), illites (10–40 MEQ/100g), chlorites (10–40 MEQ/100g), and montmorillonite (60–150 MEQ/100g). Silica is a tetrahedral structure with a silicon atom surrounded by four oxygen atoms at the same distance. The Silica tetrahedrons are joined in a hexagonal structure to replicate a sheet, as depicted in **Error! Reference source not found.** (Gunter et al., 1994).



**Figure 1**

Silica tetrahedron and hexagonal network.

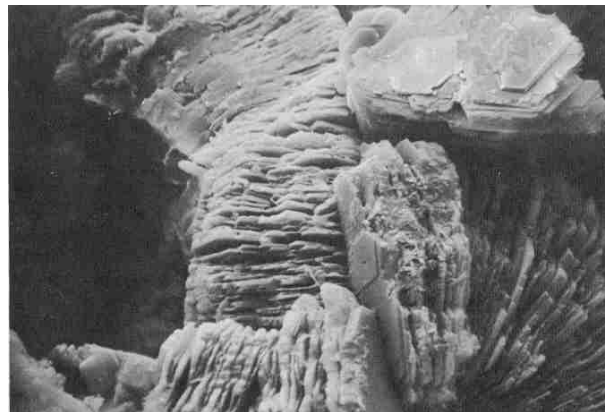
Alumina with an octahedral structure consists of an aluminum atom with six oxygen atoms arranged in an octahedron around it (**Error! Reference source not found.**). These alumina octahedrons are then joined to create a laminar structure that is the same as the Gibbsite mineral  $[\text{Al}_2(\text{OH})_6]$ .

**Figure 2**

The structural diagram of single alumina octahedron and gibbsite.

These sheets of alumina and silica are combined to form various kinds of clay.

Clays mostly encountered as drilling solids or other purposes are laminar type. The width and the thickness of these glass beads vary on the order of a micron and an angstrom, respectively, so a clay mineral width is roughly 10,000 times larger than its thickness (see **Error! Reference source not found.**).

**Figure 3**

Kaolinite mineral structure magnified about 1,600 times (Troeh and Thompson, 2005).

In the case of bentonite, as a clay mineral, this laminar structure is beneficial in filtrate-loss control (Nguyen et al., 2011).

## 2.1. The migration of fine particles and pore plugging

Fine particles in a porous medium might exist initially or be associated with injectants. These solid particles, which are at the order of molecule size (less than 1  $\mu\text{m}$ ), form colloidal solutions, and the larger ones form suspensions.

Accordingly, three varying types of damage might happen due to the migration of fine particles (Moghadasi et al., 2004):

### a. Particle exclusion

Particle exclusion or staining effect cause the particles to get stuck in pores smaller than them and not to be able to move. The staining effect is considered the simplest crucial effect that captures particles in a porous medium. **Error! Reference source not found.** demonstrates a schematic of this mechanism.

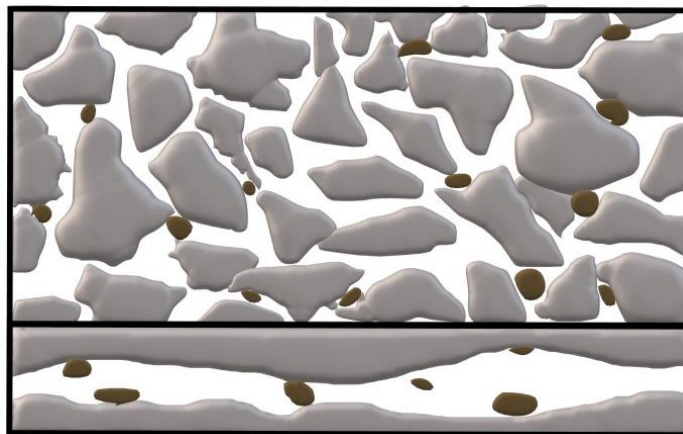


**Figure 4**

A schematic of size exclusion mechanism.

### b. Solid deposition

As shown in **Error! Reference source not found.**, the deposition of particles on pore bodies is a consequence of the migration of fine particles in which particles deposit on the pore walls. This phenomenon does not usually happen to particles smaller than pore throat size. However, it might happen stochastically (Bouddour et al., 1996).

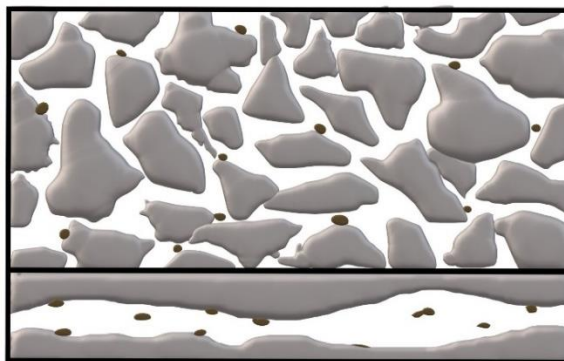


**Figure 5**

A schematic of surface deposition mechanism.

### c. Log-jamming effect or pore bridging

When particles smaller than pore throat size aggregate, they cannot pass through pores and throat. Therefore, this accumulation acts as a barrier to the fluid stream. This effect was firstly suggested by Khilar et al. (1983) for a high concentration of particles. Another possibility is that many fine particles can plug pores formed a log-jamming. The jamming ratio is the ratio of particle size and pore size. **Error! Reference source not found.** depicts the fluid trapping phenomenon in porous media due to log-jamming, the most common form of fluid trapping.

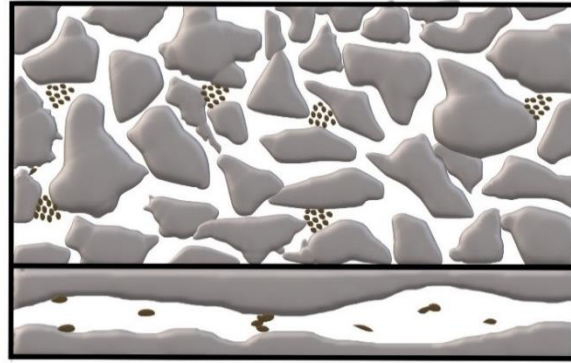


**Figure 6**

A schematic of log-jamming effect in porous media.

Many factors, such as particle and pore size distribution, mobilized and retentive forces, fluid salinity, flow rate, pore pressure, temperature, presence of organic materials, wettability, and capillary pressure control the migration of fine particles in a porous system. Aadland et al. (2018) studied different retention mechanisms during nanocellulose transport. They mentioned that adsorption and log-jamming effects happen in low salinity and high salinity water, respectively. A traditional rule was presented to determine the status of fine particles in porous media (Zhang et al., 1993).

Although many researchers attempted to describe the effect of just external or internal factors, fewer studies are allocated to a combination of both. This paper focuses on the influence of external factors such as the flow rate, applied pressure, and intrinsic properties of porous medium like grain size and the concentration of fine particles. Meanwhile, the role of the log-jamming phenomenon on permeability reduction will be discussed.

### 3. Laboratory set-up

The researchers have made a great effort to specify efficient equipment and experimental set-up to conduct this experimental work as accurately as possible. The considered test rig, shown in **Error! Reference source not found.**, was designed for this study. The test rig comprises the container, porous medium, peristaltic pump, pulsation dampener, and pressure gauges (monometer and Burdon gauge) connected to the test section.

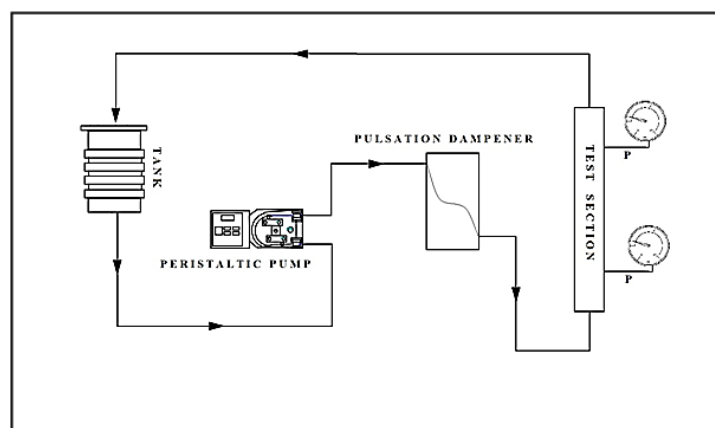


**Figure 7**

A schematic diagram of the test rig.



### 3.1. Test section

The test section, which contains the porous medium, is made of fiberglass with an internal diameter of 32 mm and a length of 580 mm. Accordingly, observing deposition and plugging processes are possible through the glass section. Six pressure taps are connected to the test section to record the pressure at different points. Nevertheless, since the permeability of the porous medium is moderately high, the pressure difference between every two adjacent gages is negligible. Hence, reported pressure in this study is an average of the six measure points. **Error! Reference source not found.** illustrates the schematic of the test section.

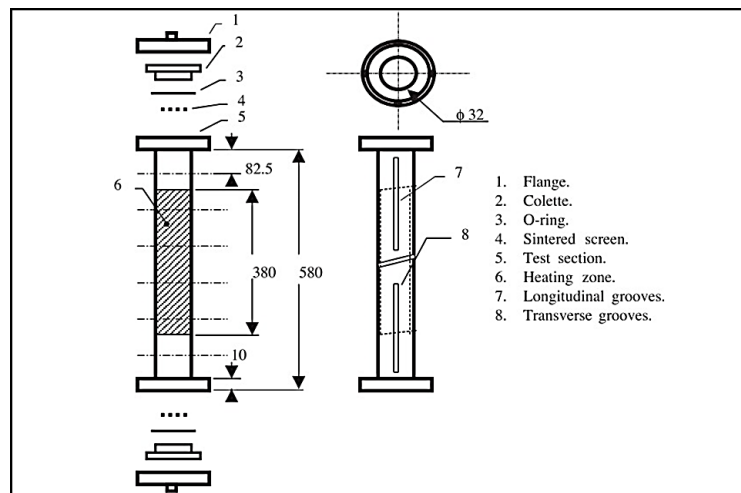


**Figure 8**

The test section design.

### 3.2. Porous medium

A sand pack composed of fine glass beads was considered the porous medium to study the migration and precipitation of suspended particles. The reason for using solid glass spheres in this study is their flowability, great strength, chemical stability, and low thermal expansion. In this study, three sand packs with different sizes of glass beads were tested to analyze the effect of grain size on migration of fine particles and permeability reduction. The glass beads used for making the sand pack were not uniform (see **Error! Reference source not found.**).

**Table 1**  
The characterization of the sand packs.

Glass bead size range ( $\mu\text{m}$ )	Mean glass bead diameter ( $\mu\text{m}$ )	Porosity	Permeability ( $\text{m}^2$ )
180–250	215	0.379	$4.41 \times 10^{-11}$
250–425	338	0.379	$7.89 \times 10^{-11}$
400–600	480	0.380	$1.59 \times 10^{-10}$

In all sand packs, the aluminum oxide was used as fine particles which can freely move in the porous system to simulate migration and precipitation of solids that belong to the porous bed, not any external source. In other words, the focus of this study is to trace the behavior of separated fine particles from rock surfaces under different circumstances. To this end, aluminum-oxide due to high resistivity to high

temperature, being inert, and availability in various sizes, which should be specified based on experimental condition, was used.

### 3.3. Peristaltic pump

The peristaltic pump, shown in Figure 9, is categorized as a positive displacement pump and pumps fluid into the porous media.

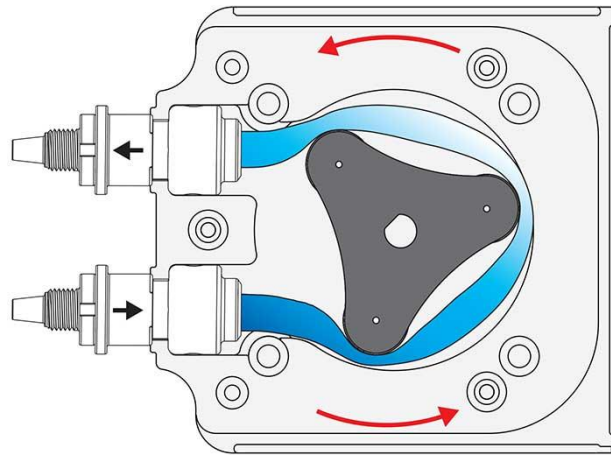


**Figure 9**

A schematic of the peristaltic pump mechanism.

Since peristaltic pumps are typically used to pump aggressive chemicals and high solids slurries, they are suitable for this study. During the tests, the flow rate remained constant to prevent pulsive flow, which is a drawback of peristaltic pumps, especially at a low rotational speed. Moreover, according to the conducted studies, pressure disturbance caused by flow rate fluctuations affects the construction and destruction of particle bridges significantly. Therefore, an additional apparatus called pulsation dampener was used too. **Error! Reference source not found.** demonstrates the calibrated rotational speed (RPM) and their corresponding flow rates used in this study.

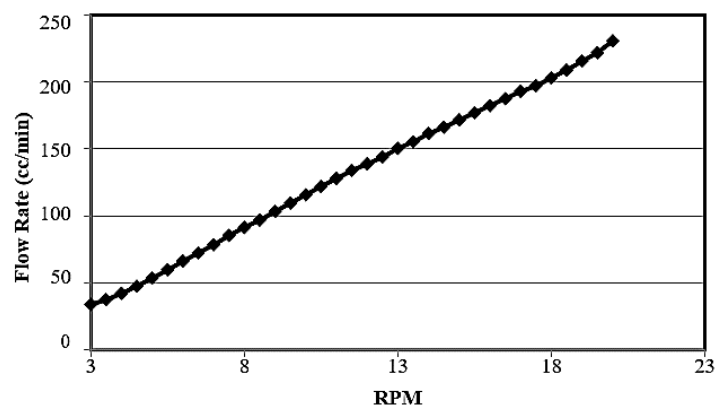


**Figure 10**

Relationship between the flow rate for peristaltic pump and the calibrated rotational speed.

### 3.4. Pulsation dampener

A pulsation dampener is an accumulator that damps system shock waves, pipe vibration, water hammers, and pressure fluctuations. Using a dampener is necessary to boost the accuracy of results and



increase the equipment lifespan. A pulsation dampener is placed downstream of the peristaltic pump. Out of quite a few kinds of pulsation dampeners, a manually designed one was used in this study because of the low operating pressure of the system (**Error! Reference source not found.**). It eliminated the fluctuations of the fluid stream by considering the compressibility of air.

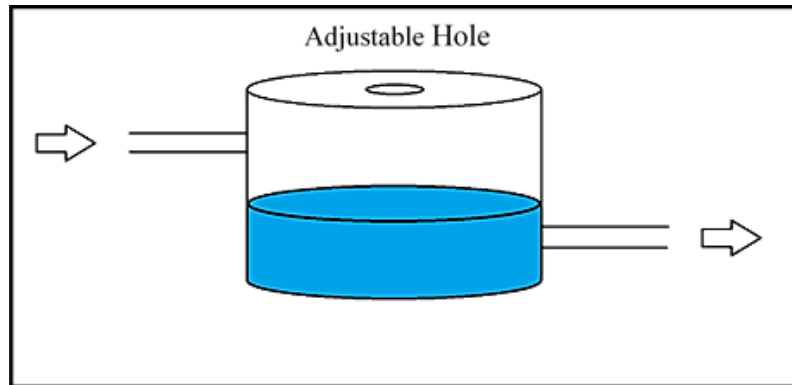


**Figure 11**

A schematic of designed pulsation dampener.

### 3.5. Pressure gauge

#### a. Manometer

As a pressure measurement device, manometers are superior to other gauges due to their high accuracy and capability of measuring low-pressure variations, just as experienced in this study. Therefore, it was used for measuring downstream pressure in this set-up.

#### b. Bourdon gauge

Unlike manometers, Bourdon gauges are designed to measure high-pressure differences. Therefore, it was set upstream according to significant pressure change in that measure-point. Fluid and equipment material compatibility should be checked to achieve accurate results because it affects outputs enormously.

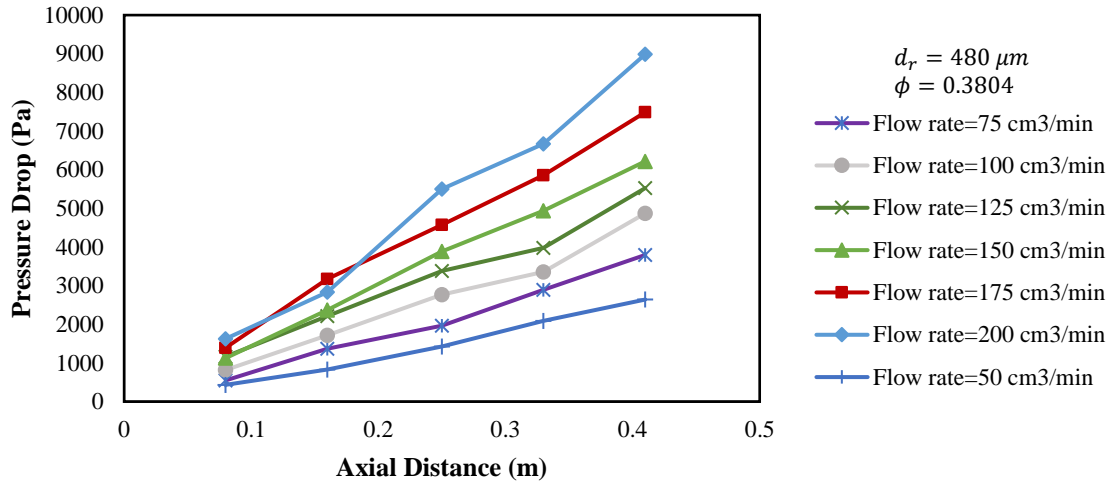
### 4. Porosity and permeability measurements

Void spaces were filled with liquid to measure the porosity of sand packs. The amount of liquid, which represents the pore volume, was divided into bulk volume (Amyx et al., 1960). Each sand pack was repeated several times to reach an average value. The results are presented in **Error! Reference source not found.**.

Absolute permeability (K) measured in the presence of single-phase fluid is closely related to pore geometry (Nan et al., 2019). Based on Darcy's equation (Equation **Error! Reference source not found.**), there is a linear relationship between pressure drop and distance from the injecting point (Kantzas et al.).

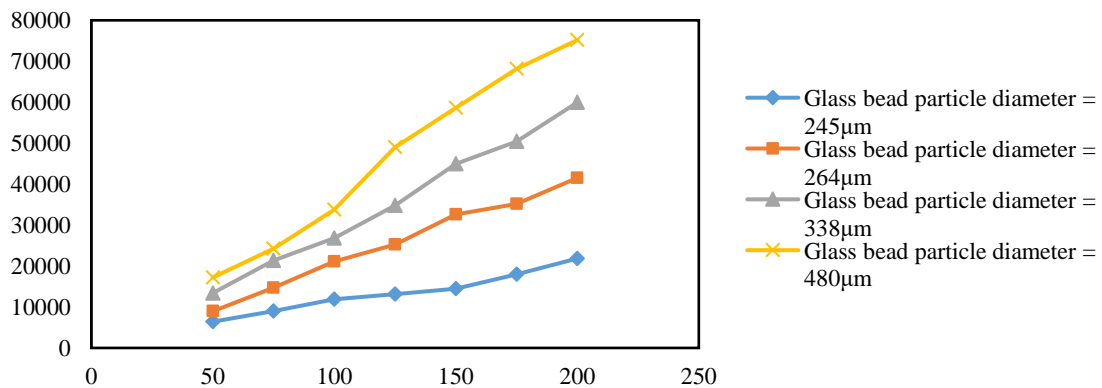
$$Q = -\frac{K_{abs}}{\mu} \left( \frac{\Delta P}{L} \right) \quad (1)$$

**Error! Reference source not found.** shows the measured pressure drop at different flow rates.

**Figure 12**

Variation of the pressure drop as a function of distance.

Measured pressure gradients at different flow rates are presented in Figure 13 to include the effect of particle size.

**Figure 13**

Variation of the pressure drop as a function of the flow rate for different glass bead sizes.

As Figure 13 demonstrates, the pressure gradient increases as solid particle size decreases. It also confirms the expected linear relationship between pressure drop and flow rate. Hence, the permeability of the porous medium can be calculated by identifying the slope of the best-fitted line on data points, employing fluid properties such as viscosity and Equation (1).

## 5. Experimental conditions

Distilled water was pumped into the test section to run preliminary tests, while pressure difference data regarding time were collected for future analysis on permeability reduction. This injection process was repeated at different flow rates. In addition, the concentration of aluminum oxide dispersed in the porous medium was changed. Similar experiments were conducted on sand packs with different bead sizes to

investigate the effect of glass bead size on permeability alteration. Table 3 presents the range of variable parameters in these experiments.

**Table 2**  
The range of operation parameters.

The temperature of injected fluid	25–30 °C
Flow rate	34–171 cm <sup>3</sup> /min
Maximum applied pressure	15 psi
The specific gravity of aluminum oxide	3.46 g/cm <sup>3</sup>
Solid particles portion of the sand pack contents	5–15 wt %
Solid particles size	7 μm

The results of this study include the influence of all essential parameters on pressure drop, and consequently, permeability reduction will be analyzed in the next section.

## 6. Results and discussion

Three parameters that significantly affect the degree of formation damage and injectivity factor were investigated in this study. They are the injection flow rate, glass bead size, i.e., porosity and permeability of the porous medium, and the concentration of fine particles dispersed initially in the porous medium.

The obtained data from these experiments were the pressure differences between two ends of the test section against time. Then, the pressure data were processed to calculate the ratio of current permeability to the original one. Pressure and permeability ratio profiles versus time at different flow rates, concentrations of suspended particles, and glass bead sizes are presented and discussed in the following sections.

### 6.1. Injection flow rate

A sand pack, composed of glass beads with a diameter of 245 μm containing 5 wt % of fine particles, was tested at various injection rates to investigate the effect of injection flow rate on pressure drop and permeability. Figures 14 and 15 show the pressure and relevant permeability ratio profiles at four different injection rates, respectively.

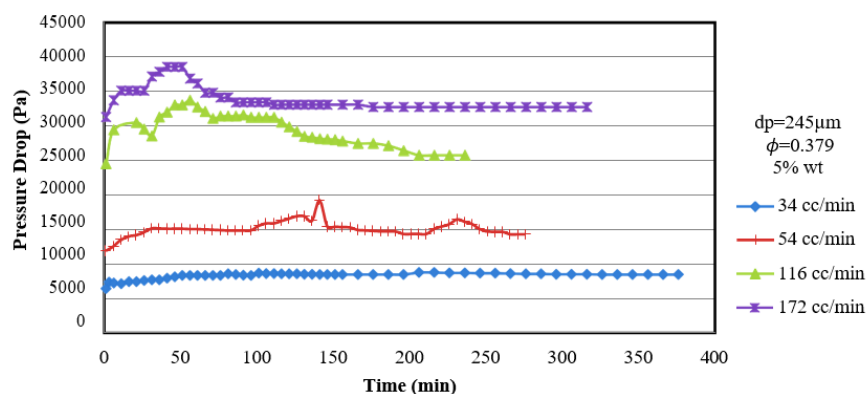


**Figure 14**

Pressure drops versus time: the effect of the flow rate variation,  $d_p = 245 \mu\text{m}$ .

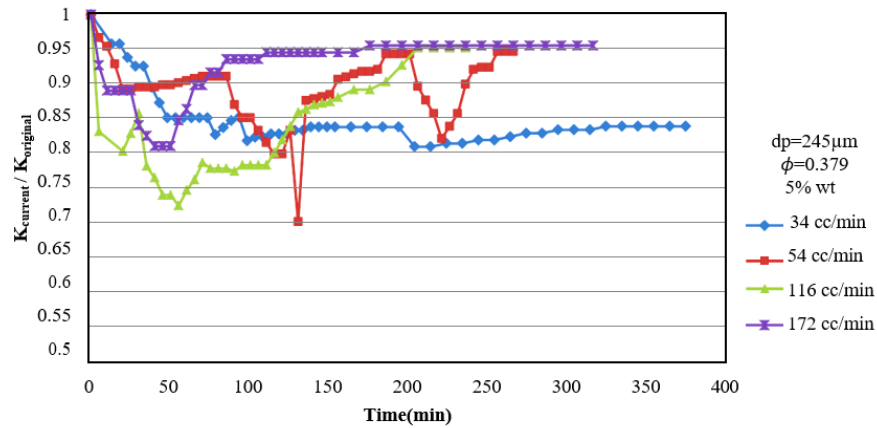


**Figure 15**

Permeability ratio versus time: the effect of flow rate variation;  $d_p = 245 \mu\text{m}$ .

Accordingly, after injecting water into the porous medium and reaching the critical velocity of particles, they spread throughout the medium and plug some throats. In these experiments, first, distilled water was pumped into the porous bed to displace the alumina particles along the fluid stream. Particles larger than pore throats and an accumulation of small particles plugged the flow paths in porous medium and diminished permeability. This reduction in permeability caused a drastic increase in the pressure gradient across the glass bead pack. A gradual increment in pressure for low flow rate cases (34 and 54 cc/min) implies that the solid particles are slowly moving, so they have time to form bridges across the pore throats.

In contrast, at high flow rates of 166 and 172 cc/min, tremendous applied pressure moved particles fast, speeding up the construction and destruction rate of bridges across pore bodies. Throat plugging reduced the cross-sectional area available to the flow stream, leading to an upsurge in the pressure drop and curtailment in absolute permeability and injectivity. After each test, all plugged media were washed with distilled water and then dried with compressed air and reassembled .

Figures 16 and 17 illustrate the same results for the different sizes of glass beads.

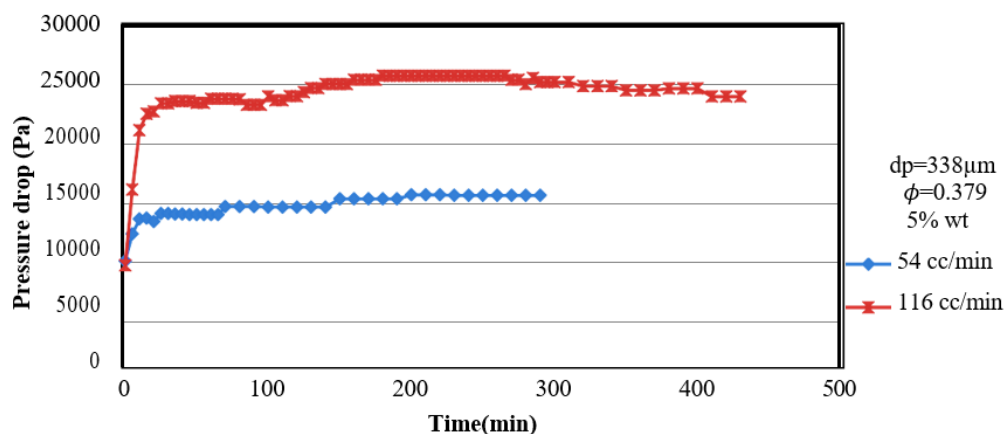


**Figure 16**

Pressure drops versus time: the effect of flow rate variation;  $d_p = 338 \mu\text{m}$ .

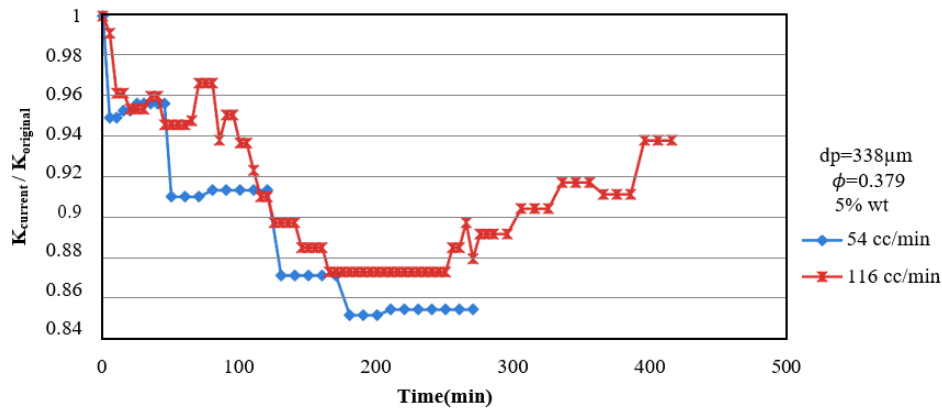


**Figure 17**

Permeability ratio versus time: the effect of flow rate variation;  $dp = 338 \mu\text{m}$ .

As presented, a cyclic increase and decrease in pressure and permeability ratio happened. The reason is that when pressure increases up to a critical value, the constructed bridges in the water path break; therefore, the pressure drop decreases. The same phenomenon was repeated for pores with larger throat sizes and led to fluctuations in the pressure drop and permeability ratio.

After a certain amount of time, the pressure reached a fixed value in all tests because fine particles in the porous medium were not transplaced anymore.

More specifically, during injection at the lowest flow rate of 54 cc/min into porous media with different glass bead sizes, it was observed that pressure drop increased gradually until reaching a constant value. According to Darcy's equation, pressure drop in a porous medium is proportional to the flow rate. However, applied pressure at this flow rate is insufficient to break the bridges and increase the cross-sectional area (see Figures 18 and 19). In other words, there is a critical flow rate below which the constructed bridges remain permanently. Hence, as shown in Figure 15, absolute permeability finally reached a specific value for all injecting rates except for the lowest one. This conclusion is valid for all glass bead sizes used in this study.

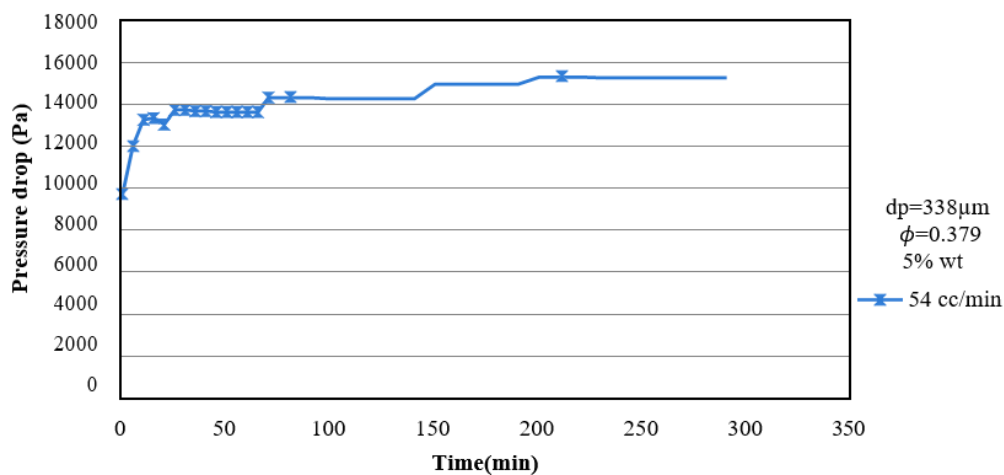


**Figure 18**

Pressure drop versus time:  $dp = 338 \mu\text{m}$  and  $q = 54 \text{ cc/min}$ .

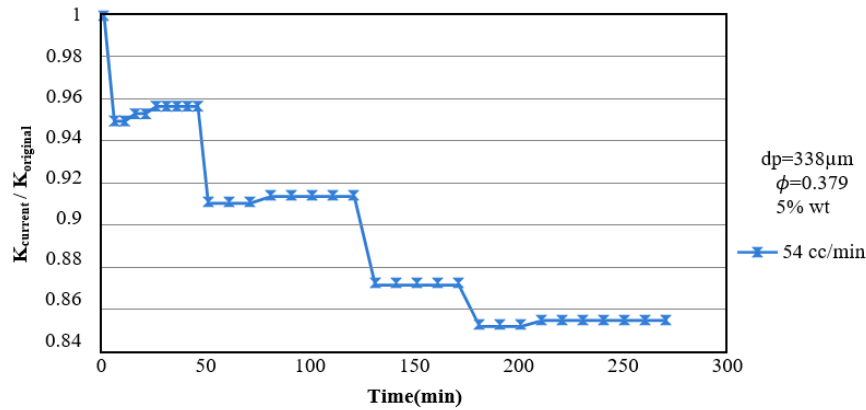


**Figure 19**

Permeability ratio versus time:  $dp = 338 \mu\text{m}$  and  $q = 54 \text{ cc/min}$ .

In all conducted experiments in this study, fine particles existed in porous media, and then pure water was injected into it. In contrast, when injected fluid contains fine particles, the results would be different (Moghadas et al., 2004). Under such circumstances, water transportation capacity diminishes, especially at the high flow rate, and fine particles deposit and form bridges more quickly, especially in the upstream section.

As explained before, there is a critical flow rate below which fine particles move forward progressively until they reach a steady state at which injected water cannot carry them any longer. In this situation, formation damage due to pore plugging reaches its highest level.

## 6.2. Glass bead size

Three sand packs with different bead sizes, as shown in Figure 20, were tested to scrutinize the impact of glass bead size. The injection flow rate was  $54 \text{ cc/min}$  for all the tests because the severest formation damage was observed at this flow rate.

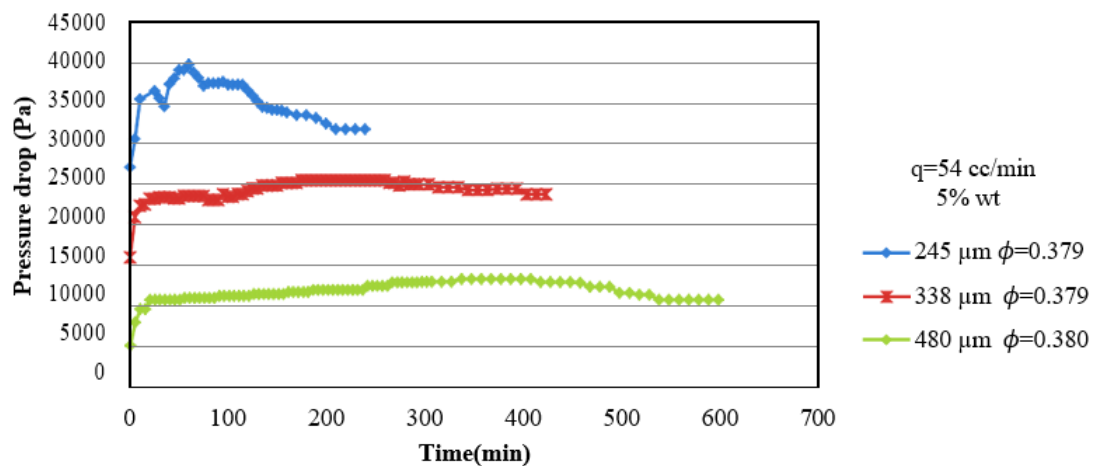


**Figure 20**

Pressure drop versus time: the effect of glass bead size;  $q = 54 \text{ cc/min}$ .

Figure 20 vividly shows that the sand pack composed of smaller glass beads reached smaller ultimate permeability because pore throat size controls absolute permeability value; therefore, blocking damage and, consequently, permeability reduction are much more intense and severe for this case (see Figure 21).

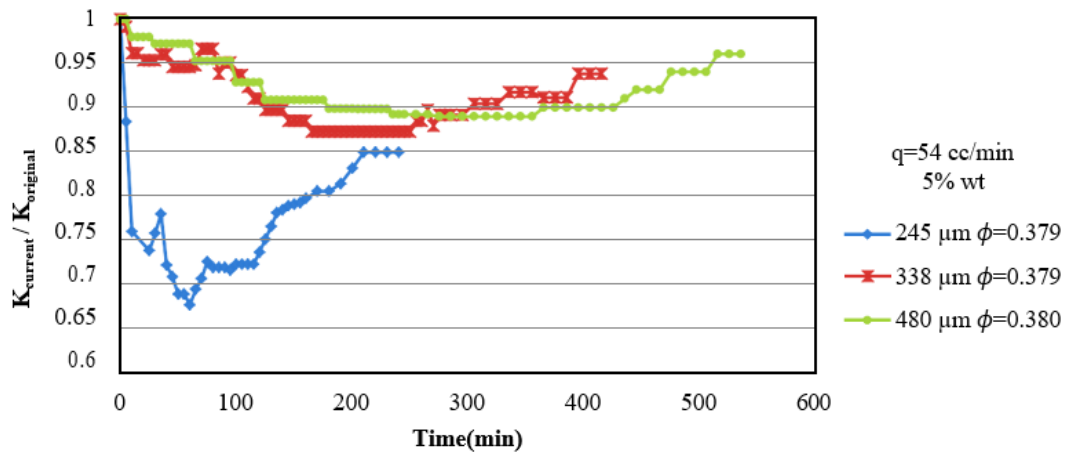


**Figure 21**

Permeability ratio versus time: the effect of glass bead size;  $q = 54$  cc/min.

Another achievement concluded from these tests is the relation between the pore plugging time and glass bead size. The smaller the glass beads are, the quicker the bridging occurs.

### 6.3. Concentration of fine particles

Fine particles may be introduced to formation inadvertently by external sources such as drilling fluids and EOR injectants or initially exist in the porous medium, just as the concerned situation studied in this paper. These fine particles can move along the flow stream due to different mechanisms: either change in hydrodynamic forces applied on loose particles or the change in the chemical properties of rock or fluid such as pH or salinity. Accordingly, fine particle movements and geomechanical deformation caused by the migration of fine particles reduce permeability and well injectivity degradation. Like previous research, due to the satisfactory properties of aluminum oxide ( $\text{Al}_2\text{O}_3$ ), it was used as fine particles in this study. Aluminum oxide, available in powder in various sizes, is inert and resistant to high temperatures.

As discussed in Section 2.1.3 and considering the employed range of glass bead size, aluminum oxide with a diameter of  $7 \mu\text{m}$  causes the log-jamming effect. Aluminum oxide with 5, 10, and 15 wt % of glass beads were put in the porous medium to examine the effect of moving solid-phase concentration on permeability alteration. Figure 22 illustrates the results of the various concentrations of fine particles on the pressure drop.



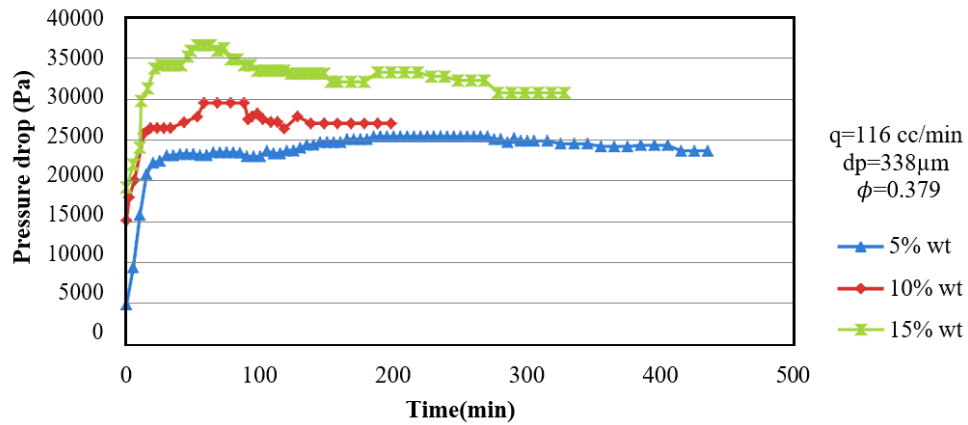


**Figure 22**

Pressure drops versus time: the effect of particle concentration;  $dp = 338$   $\mu$ m.

As illustrated in Figure 22, for a constant glass bead size (338  $\mu$ m), an increase in the concentration of fine particles led to a higher pressure drop. Accordingly, Figure 23 depicts that absolute permeability experiences more reduction at high concentrations of fine particles.

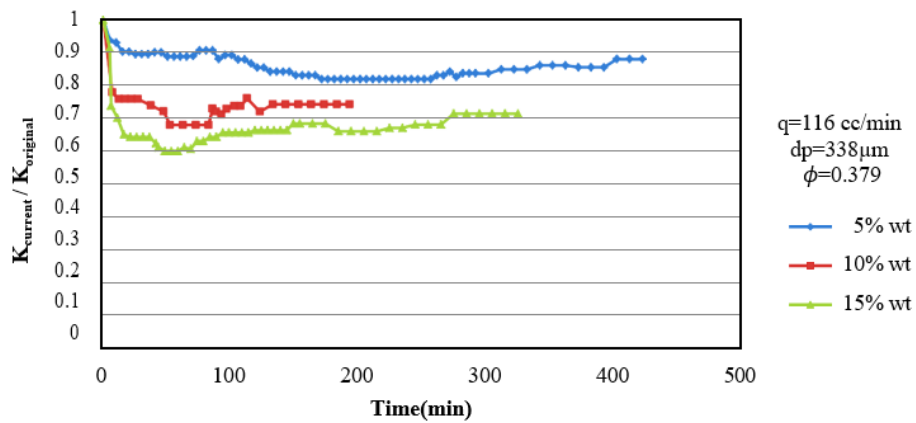


**Figure 23**

Permeability ratio versus time: the effect of the concentration of fine particles;  $dp = 338$   $\mu$ m.

## 7. Conclusions

In this study, the role of three critical parameters, namely the flow rate, glass bead size, and concentration of fine particles, in the migration of fine particles and permeability alteration was investigated. From obtained results presented in the previous section, the following statements were concluded:

- There is a critical flow rate for each porous medium below which bridges are constructed permanently. In other words, applied pressure difference on two ends of the porous medium cannot destroy them.
- The greater the absolute permeability is, the more the critical flow rate increases.

- When fine particles exist initially in the porous medium, like this study, permeability alteration due to the migration of fine particles is independent of the flow rate.
- Increasing the concentration of fine particles dispersed in the porous medium leads to severe formation damage.
- If the concentration of fine particles is maintained constant, in the case of smaller glass beads (low permeability and small pore throats), bridges are constructed faster and cause more damage.

## Nomenclature

A	Cross-sectional area (cm <sup>2</sup> )
CEC	Cation exchange capacity
d <sub>p</sub>	Glass bead size (μm)
E <sub>D</sub>	Displacement efficiency (fraction)
E <sub>V</sub>	Volumetric efficiency (fraction)
K <sub>abs</sub>	Absolute permeability (D)
L	Length of the system (cm)
MEQ	Milliequivalent
R <sub>E</sub>	Recovery efficiency (fraction)
N <sub>P</sub>	Cumulative oil production (STB)
N <sub>S</sub>	Initial oil in place before flooding (STB)
Q	Flow rate (bbl/day)
S <sub>oi</sub>	Initial oil saturation (fraction)
S <sub>or</sub>	Residual oil saturation (fraction)
S <sub>w</sub>	Average water saturation (fraction)
S <sub>wi</sub>	Initial water saturation (fraction)
T	Time (s)
U	Flow velocity (cm/s)
V	Volume (cc)
wt	Weight percent (fraction)
x	Distance (cm)
ΔP	Pressure drops along the core sample (atm)
μ	Viscosity (cP)
Φ	Porosity (fraction)

## References

- Aadland, Reidun C., Carter, J. Dziuba, Ellinor, B. Heggset, Kristin Syverud, Ole Torsæter, Torleif Holt, Ian, D., Gates, and Steven, L., Bryant., Identification of Nanocellulose Retention Characteristics in Porous Media, *Nanomaterials*, Vol. 8, No. 7, 2018.
- Alakbari, F. S., Mohyaldinn, M. E., Muhsan, A. S., Hasan, N., and Ganat, T., Chemical Sand Consolidation: from Polymers to Nanoparticles, *Polymers*, Vol. 12, No. 5, 2020.

- Amyx, J. W., Bass, D. M. and Whitin, R. L., *Petroleum Reservoir Engineering, Physical Properties*, [By] Amyx, Bass, J.W., Daniel M.,... Whiting, Robert L., McGraw-Hill Book Company, 1960.
- Bouddour, A., J. L. Auriault, and M. Mhamdi-Alaoui., *Erosion and Deposition of Solid Particles in Porous Media: Homogenization Analysis of A Formation Damage, Transport in Porous Media*, Vol. 25, No. 2, p. 121–146, 1996.
- Fanchi, J. R., *Principles of Applied Reservoir Simulation*, Principles of Applied Reservoir Simulation, 2006.
- Galal, S.K., Elgibaly, A. A. and Elsayed, S. K., *Formation Damage due to Fines Migration and Its Remedial Methods*, *Egyptian Journal of Petroleum*, Vol. 25, No. 4, p. 515–524, 2016.
- Green, Don W., and Paul Willhite, G., *Enhanced Oil Recovery*. Richardson, TX: Henry L. Doherty Memorial Fund of AIME, Society of Petroleum Engineers, 1998.
- Gulick, K. E., and William D. McCain, Jr., *Waterflooding Heterogeneous Reservoirs: an Overview of Industry Experiences and Practices*, *International Petroleum Conference and Exhibition of Mexico*, Villahermosa, Mexico, 1998.
- Gunter, W. D., Zhou, Z., and Perkins, E. H., *Modeling Formation Damage Caused By Kaolinite from 25 To 300 Degrees Centigrade in The Oil Sand Reservoirs of Alberta*, *SPE Advanced Technology Series*, Vol. 2, No. 2, p. 206–213, 1994.
- Kantzas, A., Bryan, J. and Taheri, S. *Fundamentals of Fluid Flow in Porous Media*, Calgary, University of Calgary, Canada.
- Karazincir, O., Williams, W., and Rijken, P., *Prediction of Fines Migration Through Core Testing*, *SPE Annual Technical Conference and Exhibition*, San Antonio, Texas, USA, 2017.
- Khilar, K. C., H. S. Fogler, and Ahluwalia, J. S., *Sandstone Water Sensitivity: Existence of A Critical Rate of Salinity Decrease for Particle Capture*, *Chemical Engineering Science*, Vol. 38, No. 5, p. 789–800, 1983.
- Moghadasi, J., Jamialahmadi, M., Müller-Steinhagen, H., Sharif, A., Ghalambor, A., Izadpanah, M.R., and Motaie, E., *Scale Formation in Iranian Oil Reservoir and Production Equipment During Water Injection*, *International Symposium on Oilfield Scale*, 2003.
- Moghadasi, J., Jamialahmadi, M., Müller-Steinhagen, H., Sharif, A., Izadpanah, M.R., Motaei, E., and Barati, R., *Formation Damage in Iranian Oil Fields*, *International Symposium and Exhibition on Formation Damage Control*, 2002.
- Moghadasi, J., Müller-Steinhagen, H., Jamialahmadi, M., and Sharif, A. *Theoretical and Experimental Study of Particle Movement and Deposition in Porous Media During Water Injection*, *Journal of Petroleum Science and Engineering*, Vol. 43, No. 3, p. 163–181, 2004a.
- Muecke, T. W., *Formation Fines and Factors Controlling Their Movement in Porous Media*, *Journal of Petroleum Technology*, Vol. 31, No. 2, p. 144–150, 1979.
- Nguyen, The-B., Moon-Seo, P., Jee-Hee, L., Hang-Seok, Ch., and Shin-In, H., *Characteristics of Bentonite Filter Cake on Vertical Cutoff Walls Evaluated by Modified Fluid Loss Test*, *Journal of The Korean Geotechnical Society*, Vol. 27, 2011.
- Qingjian, Li., and Prigiobbe, V., *Numerical Simulations of The Migration of Fine Particles Through Porous Media*, *Transport in Porous Media*, Vol. 122, 2018.

- Rezaei Gomari, S., and Nikhil, J., Study of The Effect of Clay Particles on Low Salinity Water Injection in Sandstone Reservoirs, *Energies*, Vol. 10, 2017.
- Satman, A., Sustainability of Geothermal Doublets, 2011.
- Sazali, Y. A., Sazali, W. M. L., Ibrahim, J. M., Graham, G., and Gödeke, S., Investigation of Fines Migration for A High-pressure, High-Temperature Carbonate Gas Reservoir Offshore Malaysia, *Journal of Petroleum Exploration and Production Technology*, Vol. 10, No. 6, p. 2387–2399, 2020.
- Sharifipour, Milad, Peyman Pourafshary, and Ali Nakhaee., Study of The Effect of Clay Swelling on The Oil Recovery Factor in Porous Media Using A Glass Micromodel, *Applied Clay Science*, Vol. 141, p. 125–131, 2017.
- Terry, Ronald E., Brandon Rogers, J., and Craft, B. C., *Applied Petroleum Reservoir Engineering*, 2015.
- Tongchao, N., Jichun, Wu., Kaixuan, Li., and Jiang, J., Permeability Estimation based on the Geometry of Pore Space Via Random Walk on Grids, *Geofluids*, No.9240203, 2019.
- Troeh, FR, and LM Thompson., *Soils and Soil Fertility*, 2005.
- Willhite, G. Paul., *Waterflooding*, 1986.
- Wright, Ch. C., and Chilingarian, G. V., Chapter 9 Water Quality for Subsurface Injection, in *Developments in Petroleum Science*, Edited By G. V. Chilingarian, J. O. Robertson and S. Kumar, Elsevier, P. 319–371, 1989.
- Zhang, N. S., Somerville, J. M., and Todd, A. C., *An Experimental Investigation of The Formation Damage Caused by Produced Oily Water Injection, Offshore Europe, Aberdeen, United Kingdom*, 1993.